



POLITECNICO
MILANO 1863

RE.PUBLIC@POLIMI

Research Publications at Politecnico di Milano

Post-Print

This is the accepted version of:

F. Toffol, S. Ricci

A Meta-Model for Composite Wingbox Sizing in Aircraft Conceptual Design

Composite Structures, Vol. 306, 2023, 116557 (13 pages)

doi:10.1016/j.compstruct.2022.116557

The final publication is available at <https://doi.org/10.1016/j.compstruct.2022.116557>

Access to the published version may require subscription.

When citing this work, cite the original published paper.

© 2023. This manuscript version is made available under the CC-BY-NC-ND 4.0 license

<http://creativecommons.org/licenses/by-nc-nd/4.0/>

Permanent link to this version

<http://hdl.handle.net/11311/1242418>

A Meta-Model for Composite Wingbox Sizing in Aircraft Conceptual Design

Francesco Toffol^{1a,*}, Sergio Ricci^a

^a*Politecnico di Milano, Department of Aerospace Science and Technology, via la Masa 34, 20156, Milano, Italy*

**Corresponding author: Francesco Toffol, francesco.toffol@polimi.it*

Abstract

This work describes the implementation of a semi-analytical representation of the wingbox structure in the conceptual and preliminary design phases, it manages different analysis and design models with different levels of detail and complexity. Starting from the description of the wing with macro-parameters, e.g. airfoils position, spar location, ribs and stringers pitch, the wing is geometrically identified and divided into its components. By providing the structural and material properties to the components, it is possible to realize different FEM models to be used for different analyses.

The introduction of the Meta-Model in conceptual design phases improves the description of the wing, providing more realistic models for the weight estimation procedure through physically based aero-servo-elastic sizing and optimization.

This approach initializes the aero-structural Digital Twin of the aircraft, which can be used for the health monitoring and maintenance planning of existing aircraft.

Keywords: *Meta-Model, Wingbox, Structural model, Digital Twin*

1. Introduction

The air transportation market is a resilient and expanding segment, with a yearly growth rate around 5% (pre COVID19). It proved its resilience with fast Revenue Per Kilometre (RPK) recovery after global crises (2008-2010), acts of terror (2001) and epidemics (Ebola, MERS). In this context, in the last years the interest towards climate changes and pollution became relevant, asking to the aviation industry to decarbonize this transportation segment. The combination of an increasing seats demand and of CO₂ emissions cut creates a challenging perspective for the next generation aircraft, which have not only to reduce but to diminish the pollution in a lively market. A simple but effective index to evaluate an aircraft performance in term of fuel efficiency is the Breguet's range equation (1): the longer is the range with a fixed amount of fuel, the lower is the fuel consumption on a given route.

$$R = \frac{V_{TAS}}{g} \left(\frac{L}{D} \right) \frac{1}{SFC} \ln \left(\frac{W_{MTOW}}{W_{MTOW} - W_{FUEL}} \right) \quad (1)$$

The Breguet's equation is dominated by three main terms which are the aerodynamic, the propulsive and the structural efficiency; across the years the focus on them evolved separately [1]. Firstly, the efficiency of the engines was improved with the High By-Pass Ratio (HBPR) turbofan (SFC term in Eq. (1)), then the evolution of the computational power initiates the Computer Aided Design (CAD) methodologies era, including CFD industrial solvers [2] (L/D term in (1)), in the last decades the spreading of composite materials reached its maximum application (>50% for the B787 [3]). The efficiency improvement season of the last 60 years seems to have reached a plateau, where the materials and designs methodologies are fully exploited but do not provide the necessary emissions cut required to satisfy FlightPath 2050 goals [4].

Since significant efficiency improvements are no more expected for the classical tube-wing configuration, in the last years many breakthrough configurations were proposed as an alternative, promising significant advantage in terms of fuel saving. They range from the more conventional High Aspect Ratio Wing (HARW), to the more challenging Strut-truss Braced wing configurations (S-TBW) like the ones studied in [5] and in [6], the boxed wing or Prandtlplane configuration like [7][8], the Blended Wing Body of [9][10][11], the Flying V of [12] and many other exotic solutions. Regardless of the future configurations adopted, it is easy to imagine that future airplanes will be characterized by greater flexibility which will make the aeroelastic design one of the most important design drivers, together with active control technologies capable of directing it. The greater deformability in fact not only can give rise to dangerous instabilities such as flutter, but also to variations in shape such as to compromise aerodynamic and flight mechanic performances.

When developing a brand-new aircraft, the conceptual and preliminary weight estimation represents a critical task, in fact it is directly involved in the computation of the overall performance of the aircraft with a snowball effect. An overestimation of the structural weight requires higher aerodynamic forces to trim the aeroplane, increasing the drag force, consequently the thrust request increases and hence the fuel consumption and the greenhouse gasses emission. On the other hand, an underestimation of the structural weight may lead to a weak structure which does not withstand the loads, or it is prone to aeroelastic instabilities which may jeopardize the aircraft safety.

The classical methodologies for the conceptual weight estimation like the one proposed by Raymer [13] and Torenbeek [14] are still based on statistical and simplified analytical methods, this does not mine their validity for conventional tube-wing aluminium configuration, but they are no more applicable for the study of unconventional configurations with composite materials simply because a sufficient statistical sample is not available. For this reason, the design methodologies must evolve concurrently with the configuration's changes, developing physical based approaches that provide realistic estimation of structural weight for new aircraft concepts. In the last 15 years the interest in conceptual design increased significantly and produced many dedicated tools for this task, like Politecnico di Milano's NeoCASS [15][16][17][18], TU-Delft's PROTEUS [19], the one proposed in [20] by You et al., the one developed by ETH and Airbus in [21], Gulfstream's ATLASS [22], the one implemented by Bombardier [23] and many others. NeoCASS is a Matlab based conceptual design environment which generates a medium fidelity fully stress sized aeroelastic model (stick FEM + VLM/DLM aerodynamic), suitable to perform from the beginning of the design loop aero-servo-elastic analysis, dynamic loads computation (trim and dynamic), flutter evaluation and active control law design for general purposes (load alleviation, flutter suppression, etc.). Indeed, this capability was considered a key requirement for future modern aircraft showing an increased flexibility, due to the use of high strength material and increased aspect ratio. However, the aeroelastic wing's design performed by the sizing module of NeoCASS, called GUESS, has some limitations for the wingbox description: indeed, the wingbox structure is represented with a rectangular and symmetric, isotropic and isostatic cross section. This description is valid to provide an initial estimation of the structural mass and it must be improved to better characterize the behaviour of modern aircraft's wings. Typically, the wingbox is not geometrically symmetric and neither for the material distribution, just as example the spar heights depends on the airfoil thickness distribution and the upper and lower skin are typically sized by different load conditions (e.g. pull-up and push-down) and characterized by different stress states, like tension, combined tension and shear or compression, able to originate buckling phenomena. Moreover, modern fibre placing techniques like tow steering allow to create coupling effects which cannot be neglected in aeroelastic sizing, but they are not included in the stick model currently adopted by GUESS to describe the wingbox of aircraft's lifting surfaces.

This work presents an enhanced approach to the wingbox description from its geometrical and structural point of view through the so-called Meta-Model, it allows to improve the characterization of the wing and it can be exploited in the conceptual and preliminary design phases considering arbitrary sections and material distributions for the sizing. The lacks in the current wingbox description are filled, allowing to describe arbitrary sections with heterogeneous and orthotropic materials. Thanks to the semi-analytic formulation here adopted it is possible to

characterize the wingbox with a centralized database that is interfaced with different analysis models and representation of the wingbox.

The aeroelastic effects introduced with composite orthotropic materials e.g., aeroelastic tailoring, must be considered since the early design phases to have a realistic estimation of the component's stiffness, masses, and applied loads. However, high fidelity analysis and optimization capabilities are not compatible with the many aircraft configurations that must be analysed in the conceptual design phase, to select two/three best candidates to be moved on to the preliminary and detailed design phases. Moreover, the transferring of the conceptual design results to the next design phases must be implemented in a smooth, reliable, and fast way. For example, the high-fidelity analyses performed in detailed design phase, like [24][25][26][27], can be facilitated if the GFEM/CAD models are the automatized outputs of previous design steps. The load applied are computed with physical based approach on realistic FEM stick model that accounts for the composite effects in the aeroelastic loads computation. A unique representation of the wingbox through the Meta-Model is useful also to condensate high-fidelity results into a simple stick model, which is still the reference representation of the aircraft for the load computation.

In recent years, the interest towards the aircraft digitalization is increased and the so called Digital Twin (DT) gained a relevant role in aircraft design and life cycle operation [28][29][30]. The digital twin concept was born in a military environment, where the shrink of defence budgets introduced a life extension program of the existing aircraft that must reduce the maintenance costs. The combination of these two factors generated the development of a digital equivalent model of each real aircraft identified by its tail number (TN), through which it is possible to recover the stress information starting from the mission profile accomplished by the aircraft and evaluate the fatigue of the components. This approach can be extended to the whole disciplines involved in the aircraft life cycle like design, production, operation and dismissing, at different levels of detail and complexity.

The Meta-Model of the wingbox here proposed can be considered as the first brick toward the Digital Twin of the conceptual aircraft for the entire aero-servo-elastic domain, starting from the initial sizing, until the more complex aeroelastic analyses with and without active control systems.

2. The Wingbox Meta-Model concept

The Meta-Model is a semi-analytical three-dimensional representation of the wingbox that contains both geometrical and structural information. The Meta-Model recalls the approach proposed in [31], further developing the geometrical description and modifying the computational method for beam stiffness matrix evaluation.

The Meta-Model is not a simple collection of information, but thanks to its analytical implementation it can rearrange them to create and update different analysis models and to post-process analysis results, assuming a pivotal role in the models' management and information exchange (Figure 1)

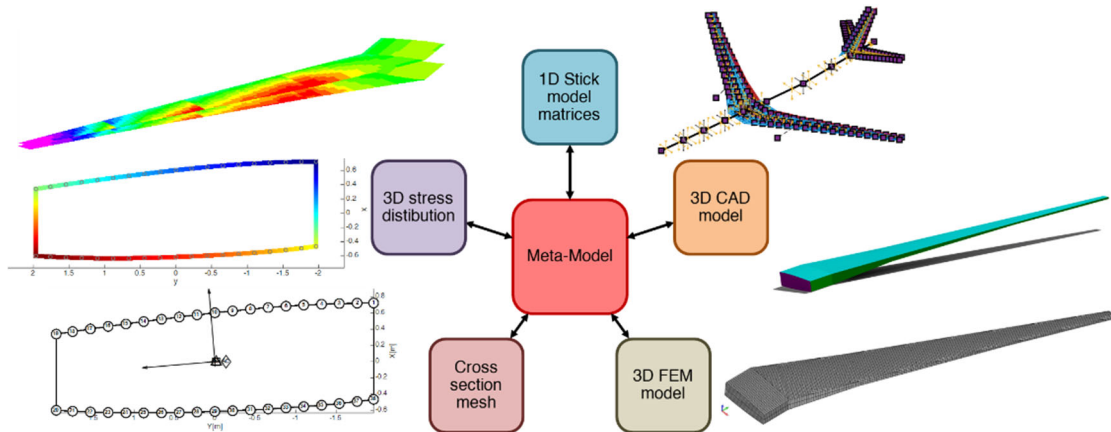


Figure 1: Meta-model environment

The wing layout is inherited from the model realized with AcBuilder, the geometrical environment of NeoCASS, where the wing is described in term of macro parameters like airfoils, span, dihedral and sweep angles, taper ratio and wingbox dimensions and position, providing a graphical representation as in Figure 2a. The model is hence imported in NeoCASS and the wing's characteristics processed to describe the wing as a ruled surface defined by a set of airfoils (Figure 2b). At this point, it begins the identification on the wingbox performed by the Meta-Model: a set of planes representing the front and rear spar is used to crop the wingbox, obtaining its external surface (Figure 2c).

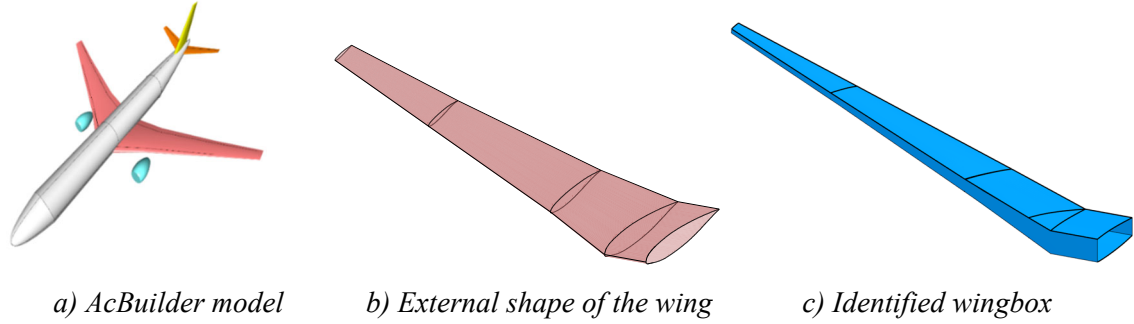


Figure 2: Different representations of the wing, from AcBuilder to the identified wingbox

The realization of the Meta-Model continues with the identification of the remaining geometrical information, which are the intersections among the ribs and the stringers. To do that, a set of planes normal to the beam axis (Figure 3a), with a user defined spacing, is used to draw the perimeter of all the ribs except the ones in the kink region. Now it is stringers' turn, which are identified intersecting the ribs with a set of parallel and equally spaced planes (Figure 3b). It is possible to use three alignments for the stringer: 1) parallel to front spar 2) aligned with the beam axis 3) aligned with the rear spar.

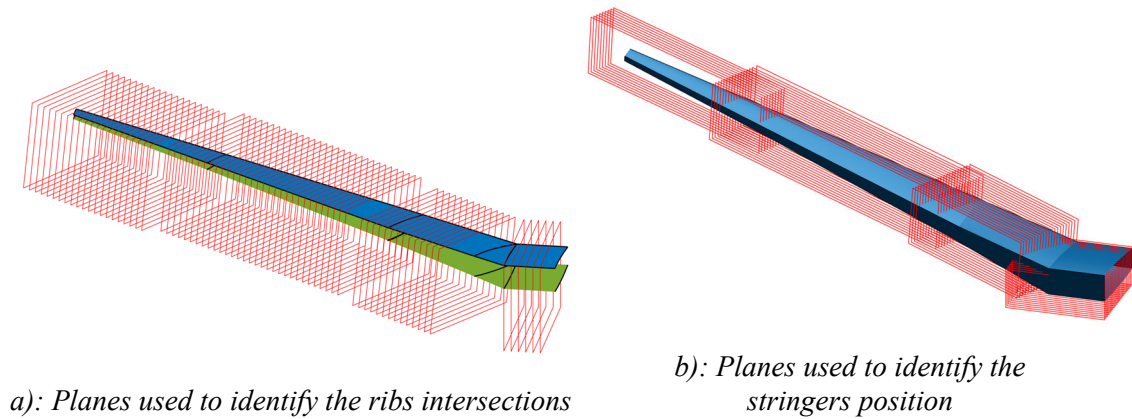


Figure 3: Planes used to identify ribs and stringers layout

The last step for the full description of the wingbox geometry is the modelling of the kinks, which is automatically performed placing additional semi-ribs if the distance between the two ends of the kink is too wide, the additional ribs are placed in such a way that they match a stringer on the inner rib, as in Figure 4. This last feature is needed to avoid automatic meshing problems in the kink area.

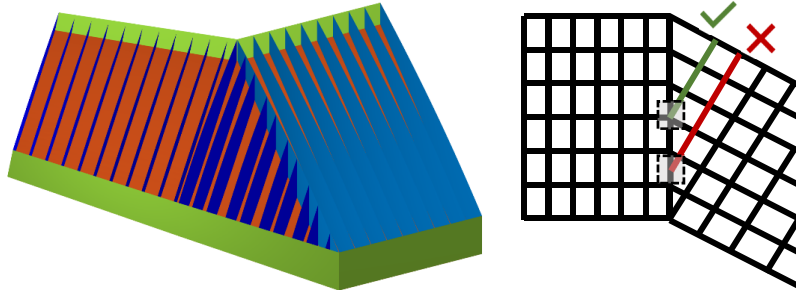


Figure 4: Detail of the kink CAD (left) and mid kink rib positioning (right)

This cut and intersect process is coded in Matlab, modelling the surfaces with triangular patches and exploiting the intersection method described in [32] and implemented in [33]. After this geometrical pre-processing, the Meta-Model links material properties, and thicknesses to the structural elements, fully describing each component. Different levels of connectivity among the points generate two FEM models and the CAD models in “iges” or “CATIA” format. The first FEM model realized is the Nastran-like Global FEM of the wingbox (GFEM), three refinement directions can be exploited to modify the number of elements in chord, span and thickness directions. The planar structural elements are modelled with triangular (CTRIA) and rectangular (CQUAD) shell elements, with the properties defined by PSHELL for isotropic components and PCOMP for orthotropic ones. The stringers are modelled with 1D beam elements (PBAR). An example of the obtained model is represented in Figure 5.

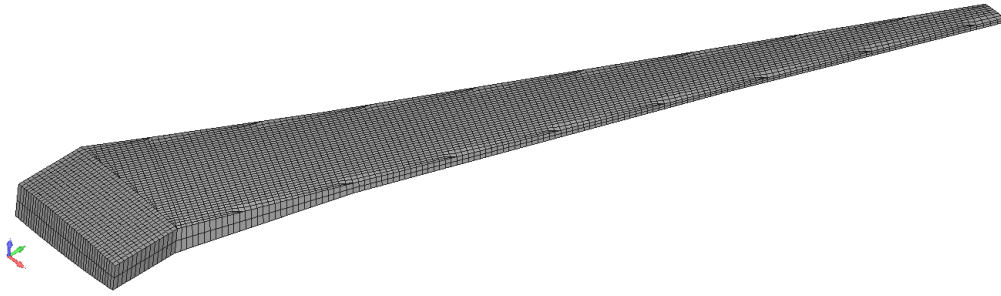


Figure 5: 3D FEM of the wingbox realized with the Meta-Model

The second FEM model realized exploits the connectivity in chordwise direction on each rib, creating a 2D cross sectional FEM model which is analysed with the dedicated module NeoANBA: it is a FE cross sectional solver which provides the stiffness and mass matrices of an arbitrary anisotropic beam section together with its stress distribution under external loading, its description is demanded to the dedicated section 3. Most important, NeoANBA is the mean to automatically generate, starting from the 3D FEM model of the wingbox, the typical reduced order model, also called stick model, based on beams elements, used for aircraft dynamic and aeroelastic analysis.

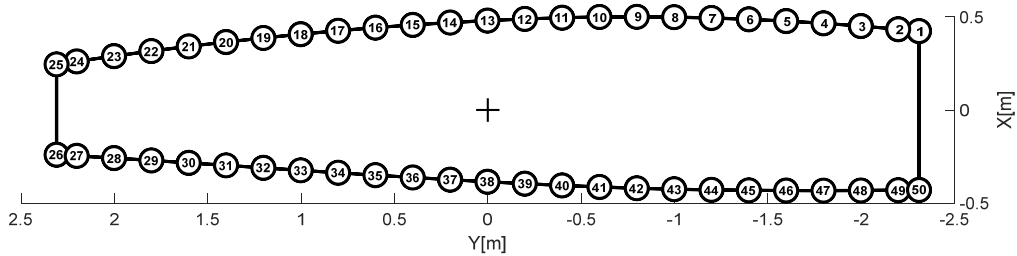


Figure 6: Example of a NeoANBA cross-section FE mesh

The Meta-Model re-arranges the connectivity to create two different CAD files which can be used to build other FEM models or to perform fitting study of the wingbox with the other wing systems e.g. landing gear, slats, flaps, etc. The first model is realized using a VBA macro: the Meta-Model writes the macro that is run by CATIA, building the parametric model inside the CAD environment. The second model exploits the NURBS [34] to write an equivalent IGES standard file. In both cases a result like the one of Figure 7 is produced.

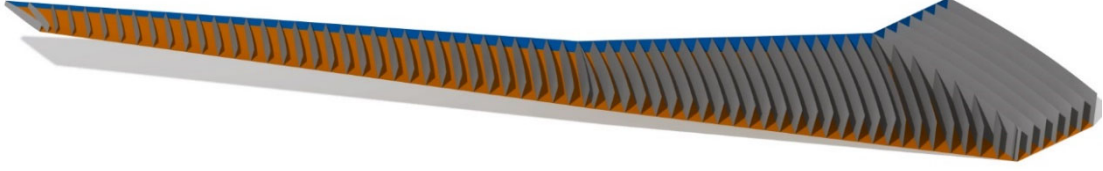


Figure 7: CAD model of the wingbox

The Meta-Model does not only realise different models, but it also allows the communication between them and organize the information flow, for example in the aeroelastic sizing process. As shown in Figure 1 the Meta-Model is interfaced with all the models and whichever variation, e.g. the thickness of a skin, is automatically mapped in all the analysis domains. This feature is important when the Meta-Model is exploited in an optimization environment like NeOPT [35], which is the new optimization suite implemented in NeoCASS. The physical design variables like thicknesses are modified by the optimization algorithm and the analysis models are updated thanks to the Meta-Model.

Briefly summarizing the optimization process, at each iteration the structural properties (design variables) are updated and the beam properties of the stick model re-computed, the aeroelastic simulation provides the loads and other responses used as constraints (e.g. flutter). The results in terms of internal forces are processed by NeoANBA to obtain the sectional stress state which is used to evaluate the structural design constraints, such as maximum allowable stresses and strains or buckling loads. The information exchange is possible and managed by the Meta-Model.

3. NeoANBA

NeoANBA is the name of the cross-sectional Finite Element solver used by the Meta-Model to evaluate the beam structural matrices and to recover the sectional stresses, the name itself is the combination of NeoCASS and ANBA, since it was developed to improve the beam description of the stick model exploited in the NeoCASS aeroelastic suite re-implementing the Anisotropic Beam theory described in [36]. This was necessary to have all the features in the same programming language and avoid calls to external solvers.

The main motivation behind the development of this solver is the need to obtain a cross sectional stiffness matrix which is non-sensitive to the topology of the section, e.g. multiple spar configuration, and to evaluate the coupling terms introduced by orthotropic materials. Analytical solutions for multiple cells isotropic section are available [37][38], but they provide an evaluation of the stiffness matrix that account only for diagonal terms and terms due to shear centre and neutral axis offsets, leading to a cross section stiffness matrix in the form of Eq.(2)

$$K = \begin{bmatrix} G \times A_x & & & & & G \times A_x \times X_{SC} \\ & G \times A_y & & & & -G \times A_y \times Y_{SC} \\ & & E \times A & -E \times A \times X_{NA} & E \times A \times Y_{NA} & \\ & & & E \times J_{xx} & & \\ & SYM & & & E \times J_{yy} & \\ & & & & & G \times J_t \end{bmatrix} \quad (2)$$

It must be noticed that the matrix elements are the multiplication of material properties (E, G) and geometrical properties (A, J, X_{ij}). This formulation is representative of isotropic sections, but when composite materials are used, extra diagonal terms (coupling) are no longer null and an analytical solution for their estimation is not available. The problem was faced starting from the '80, when the interest in composite helicopter blade sections fostered the development of methodologies for the cross-section stiffness evaluation, like the aforementioned ANBA and VABS [39].

The (Neo)ANBA formulation [41] is based on the kinematic assumption that the cross section is not rigid and the displacement of one point $\mathbf{s}(x, y, z)$ can be decomposed into a rigid section motion $\mathbf{v}(z)$ (three rigid displacements and three rigid rotations of the beam line) and a warping field $\mathbf{g}(x, y, z)$ (Figure 8 and Eq. (3))

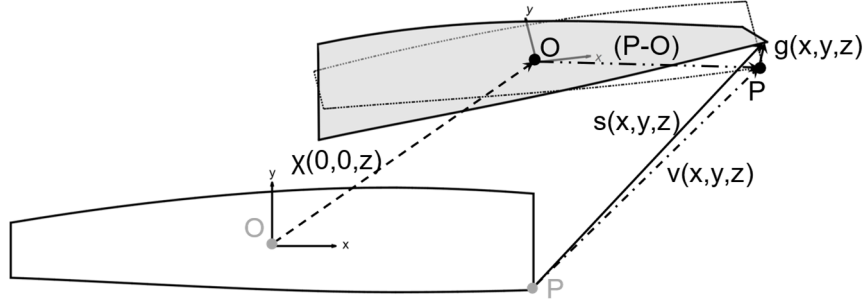


Figure 8: Kinematics of the cross-section

$$\begin{aligned} \mathbf{s}(x, y, z) &= \boldsymbol{\chi}(z) + [(\mathbf{P} - \mathbf{O}) \times^T] \boldsymbol{\varphi}(z) + \mathbf{g}(x, y, z) = \mathbf{v}(z) + \mathbf{g}(x, y, z) = \\ &= \mathbf{Z}(x, y) \mathbf{r}(z) + \mathbf{g}(x, y, z) \end{aligned} \quad (3)$$

The total displacement is partitioned along the section reference system principal direction $\mathbf{s}(x, y, z) = [u \ v \ w]^T$, the model considers all the strain components $\boldsymbol{\varepsilon} = [\gamma_{xy} \ \varepsilon_x \ \varepsilon_y \ \gamma_{xz} \ \gamma_{yz} \ \varepsilon_z]^T$ and the energetically conjugated stresses $\boldsymbol{\sigma} = [\tau_{xy} \ \sigma_x \ \sigma_y \ \tau_{xz} \ \tau_{yz} \ \sigma_z]^T$. The relation between the stress and the strain vectors is provided by the constitutive law so that $\boldsymbol{\sigma} = \mathbf{C} \boldsymbol{\varepsilon}$.

The strains are obtained from the displacement through a derivative process, that is divided into the derivative on the cross-section plane \mathbf{D}_{xy} and along the section normal $(\cdot)_{\partial z}$, leading to Eq.(4) where \mathbf{S} is an extraction matrix

$$\boldsymbol{\varepsilon} = \mathbf{D}_{xy} \mathbf{s} + \mathbf{S} \mathbf{s}_{\partial z} \quad (4)$$

The strain vector can be divided in two components as in Eq.(5), one due to the rigid section displacement $\boldsymbol{\varepsilon}_r$ and the other due to the warping $\boldsymbol{\varepsilon}_g$:

$$\boldsymbol{\varepsilon} = \boldsymbol{\varepsilon}_r + \boldsymbol{\varepsilon}_g = \mathbf{D}_{xy} \mathbf{Z} \mathbf{r} + \mathbf{S} \mathbf{Z} \mathbf{r}_{\partial z} + \mathbf{D}_{xy} \mathbf{g} + \mathbf{S} \mathbf{g}_{\partial z} \quad (5)$$

The kinematics of the section must describe a rigid motion, which requires $\boldsymbol{\varepsilon}_r = \mathbf{0}$. The non-null components of the rigid strain vectors are $\boldsymbol{\varepsilon}_r^N = [\gamma_{xz} \ \gamma_{yz} \ \varepsilon_z]$, which are obtained as in Eq.(6)

$$\boldsymbol{\varepsilon}_r^N = \mathbf{t} \boldsymbol{\varphi} + \boldsymbol{\chi}_{\partial z} + [(\mathbf{P} - \mathbf{O}) \wedge]^T \boldsymbol{\varphi}_{\partial z} \quad \text{with} \quad \# = \begin{bmatrix} 0 & -1 & 0 \\ 1 & 0 & 0 \\ 0 & 0 & 0 \end{bmatrix} \quad (6)$$

The system of two equations of Eq.(7) guarantees that the rigid strains are null everywhere across the section, the first equation guarantees $\varepsilon_r^N = 0$ for $(x, y) = 0$, the second one imposes the same condition for $\forall(x, y) \neq 0$

$$\begin{bmatrix} 0 & t \\ 0 & 0 \end{bmatrix} \begin{bmatrix} \chi \\ \varphi \end{bmatrix} + \begin{bmatrix} \chi \\ \varphi \end{bmatrix}_{\partial z} = \mathbf{T}\mathbf{r} + \mathbf{r}_{\partial z} = \mathbf{0}\# \quad (7)$$

If Eq.(7) is satisfied, then the reference line motion is rigid, otherwise the result provides an indication of how far the displacement is from a rigid one. Indeed, the equation becomes $\mathbf{T}\mathbf{r} + \mathbf{r}_{\partial z} = \mathbf{\Psi}$, with $\mathbf{\Psi}$ that is the generalized strain parameter. In this way, the rigid strain can be re-written as $\varepsilon_r = \mathbf{S}\mathbf{Z}\mathbf{\Psi}$

It is now possible to specialize the Virtual Work Principle (VWP) for unit length, considering a beam chunk with constant cross-sectional area, null lateral surface, null volume forces and loaded at its ends by the pressure vector \mathbf{p} . The VWP becomes Eq.(8).

$$\int_A \delta \varepsilon^T \boldsymbol{\sigma} dA = \int_A (\delta \mathbf{s}^T \mathbf{p}_{Az})_{\partial z} dA\# \quad (8)$$

It is possible to consider the internal forces as the resultant of the stresses acting on the cross-section, namely $\boldsymbol{\theta} = \int_A \mathbf{Z}^T \mathbf{p} dA = [T_z \ T_x \ T_y \ M_x \ M_y \ M_z]^T$.

All the equations are written in the continuous space domain; to solve the problem numerically a Ritz's like approach is used. The shape functions \mathbf{N} are used to approximate the warping field for both its virtual variation and for the unknown field, providing a Bubonov-Galerkin projection of the problem on a space having the \mathbf{N} shape function as base. With this approach, the warping field becomes $\mathbf{g} = \mathbf{N}\mathbf{a}$, with \mathbf{a} the unknown vector of nodal warping. NeoANBA uses conventional FEM approach to the problem with iso-parametric elements. The displacement becomes $\mathbf{s} = \mathbf{Z}\mathbf{r} + \mathbf{N}\mathbf{a}$ and leads to the strain expression of Eq.(9)

$$\varepsilon = \mathbf{S}\mathbf{Z}\mathbf{\Psi} + \mathbf{D}_{xy}\mathbf{N}\mathbf{a} + \mathbf{S}\mathbf{N}\mathbf{a}_{\partial z} = [\mathbf{B}_{\Psi} \ \mathbf{B}_a \ \mathbf{B}_{a\partial z}] \begin{bmatrix} \mathbf{\Psi} \\ \mathbf{a} \\ \mathbf{a}_{\partial z} \end{bmatrix} = \mathbf{B}\mathbf{q}\# \quad (9)$$

The internal virtual work becomes $\delta W_{internal} = \delta \mathbf{q}^T \int_A \mathbf{B}^T \mathbf{C} \mathbf{B} dA \mathbf{q} = \delta \mathbf{q}^T \mathbf{W} \mathbf{q}$. \mathbf{W} is the 3x3 block symmetric matrix of Eq.(10) and is the result of the numerical integration of the $\delta W_{internal}$, performed using the Gauss's quadrature scheme for example.

$$\mathbf{W} = \begin{bmatrix} \bar{K} & \hat{R}^T & \tilde{R}^T \\ & \hat{K} & \hat{H} \\ sym. & & \tilde{K} \end{bmatrix}\# \quad (10)$$

The external work can be re-written as $\delta W_{external} = \delta \mathbf{a}_{\partial z}^T \mathbf{P} + \delta \mathbf{a}^T \mathbf{P}_{\partial z} + \delta \mathbf{r}^T (\boldsymbol{\theta}_{\partial z} - \mathbf{T}\boldsymbol{\theta}) + \delta \mathbf{\Psi}^T \boldsymbol{\theta}$ and it is now possible to write the discrete VWP In matrix form as:

$$\begin{bmatrix} \delta \mathbf{\Psi} \\ \delta \mathbf{a} \\ \delta \mathbf{a}_{\partial z} \\ \delta \mathbf{r} \end{bmatrix} \left(\begin{bmatrix} \bar{K} & \hat{R}^T & \tilde{R}^T & 0 \\ & \hat{K} & \hat{H} & 0 \\ sym & & \tilde{K} & 0 \\ 0 & 0 & 0 & 0 \end{bmatrix} - \begin{bmatrix} \boldsymbol{\theta} & \mathbf{P}_{\partial z} & \mathbf{P} \\ \boldsymbol{\theta}_{\partial z} - \mathbf{T}^T \boldsymbol{\theta} \end{bmatrix} \right) = \mathbf{0}\# \quad (11)$$

Imposing the arbitrariness of the VWP, two sets of equations are obtained. The first set is obtained imposing $\delta \mathbf{r} = 1$ and null the other virtual variations, obtaining the known differential property of the internal load as $\boldsymbol{\theta}_{\partial z} - \mathbf{T}^T \boldsymbol{\theta} = \mathbf{0}$. Vice-versa, imposing all the variation as unit and null reference line motion, the governing equations of the problem are obtained. Thanks to the

differential property of the internal loads, it is possible to assume their linear variation along the beam axis:

$$\begin{cases} \theta(z=0) = \theta_0 \\ \theta(z) = (I + zT^T)\theta_0 \end{cases} \quad (12)$$

The assumption done in Eq.(12) is extended to all the other unknowns of the problem $\mathbf{X}(z) = (\mathbf{C}_0 + z\mathbf{C}_1)\theta_0$, leading to:

$$\begin{bmatrix} \bar{K} & \hat{R}^T & \tilde{R}^T \\ & \bar{K} & \hat{H} \\ sym. & & \tilde{K} \end{bmatrix} \begin{bmatrix} \Psi_0 + z\Psi_1 \\ A_0 + zA_1 \\ A_1 \end{bmatrix} = \begin{bmatrix} I + zT^T \\ P_1 \\ P_0 + zP_1 \end{bmatrix} \# \quad (13)$$

Eq.(13) is solved in two steps, the first one for $\forall z$ and the second one for $z = 0$. Recalling Eq.(9) the strain vector becomes $\boldsymbol{\varepsilon} = (\mathbf{B}_\Psi \Psi_0 + \mathbf{B}_a \mathbf{A}_0 + \mathbf{B}_{a\partial z} \mathbf{A}_1) \theta_0$, which is linear in θ_0 and can be solved for unit internal loads. Rewriting the external virtual work as $\delta W_{external} = \delta \theta_0^T \Psi_0 = \delta \theta_0^T \mathbf{K}_{sec}^{-1} \theta_0$, the cross-section stiffness matrix becomes $\mathbf{K}_{sec} = (\mathbf{A}_1^T \mathbf{P}_0 + \mathbf{A}_0^T \mathbf{P}_1 + \Psi_0^T)^{-1}$.

The method can be specialized to different element types, as it is done in classical FEM solution. In the case of a wingbox, the skins and the webs are mainly loaded with shear and axial loads, while the stringers and spar caps withstand the axial force introduced by the bending moments, the behaviour of these structural elements suggests the development of two different element types to describe the components: the first element has to describe the membranal behaviour of the planar structures while the second one has to model the axial response of the longitudinal components. If composite laminate materials are used, the elemental stiffness matrix is computed with the Classical Lamination Theory (CLT), specialized for planar stress state.

The iso-parametric panel element is a two nodes element which account only for the axial and the transverse shear, simplifying the constitutive law, and accounting only for the warping normal to the cross-section. The stringer element is a concentrated stiffness element that accounts for the axial deformation of a point with a concentrated area.

These two elements are sufficient to describe a thin-walled hollow section, typical not only of the wingbox, but of many other aeronautical structures like fuselage or rocket fuel tanks.

The cross-sectional solver has been validated with different test cases, from the simplest rectangular section to realistic wing cross-section.

The first validation test is performed benchmarking the results obtained with NeoANBA and the one of [36]. The rectangular section is 600mm x 100mm and has three stringers equally spaced on the two long edges as illustrated in Figure 9.

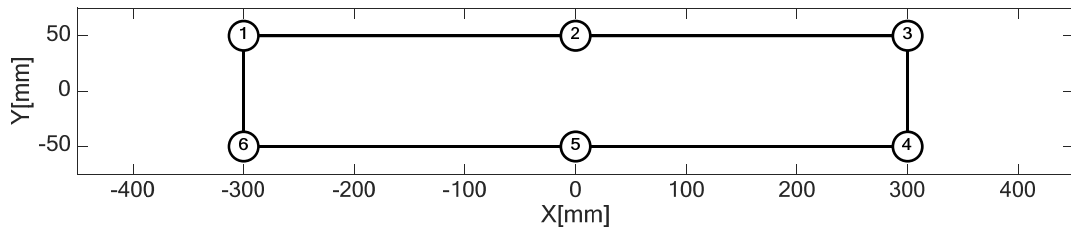


Figure 9: Cross section used to validate NeoANBA

The material properties of the aluminium alloy used for the components are reported in Table 1.

E[Mpa]	G[Mpa]	$\nu[-]$
73800	28100	$\frac{E}{2G} - 1 = 0.3132$

Table 1: Material properties for the validation case

The 1mm skins withstand only shear stresses while the 200mm² stringers resist the axial stress (z direction).

The results obtained with NeoANBA are compared with the analytical solution for six different load cases (3 orthogonal forces F_x , F_y , F_z and 3 orthogonal moments M_x , M_y , M_z). The axial stresses in the stringers are generated by the two out of cross-section moment and the axial force (M_x , M_y , F_z) while the shear stresses in the panels are due to the torsional moment and the two in-plane shear forces (M_z , F_x , F_y).

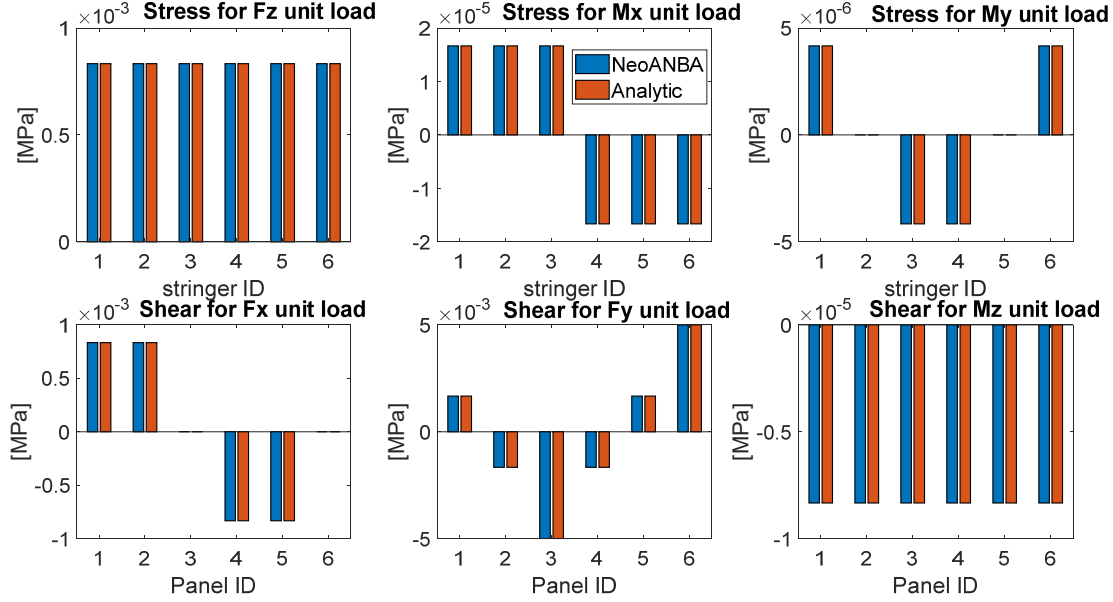


Figure 10: Axial stress in the stringers (top) and shear stress in the panel (bottom), NeoANBA vs. analytical solution

The results in Figure 10 show that the axial and shear distribution obtained with NeoANBA are identical to the ones obtained analytically.

4. Meta-Model and NeoANBA validation

A further mean of validation of NeoANBA and its implementation inside the Meta-Model is hereafter presented. A rectangular and non-tapered wingbox is realized exploiting the Meta-Model, among the available outputs of the procedure there is the realization of a detailed 3D FEM model, which is used as reference in the following. The same wingbox is represented with a stick model, whose beam stiffness matrices are computed with NeoANBA.

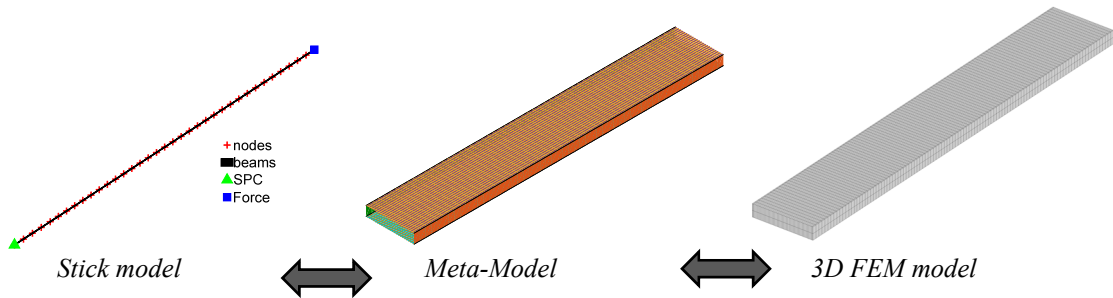


Figure 11: Visualization of the models employed in the validation phase

The two models are clamped at one end and loaded with a force or moment on the free end. The quantities of interest of the comparison are the displacements, which assesses the stiffness matrix

estimation capability of the cross-sectional solver, and the stress distribution, that assesses the quality of the stress recovery obtained with NeoANBA.

Two cases are selected to validate the model, a load normal to the wing surface i.e. in lift direction and a torsional moment around the beam axis. In the first case the displacement components to be monitored are the ones in the force direction, Figure 12 shows how the deformed shapes obtained with the stick model and the 3D FEM model are equivalent both for the vertical component TZ and for the rotation RX. In the comparison in Figure 13, Figure 14 and Figure 16 the pattern on the left is obtained with the GFEM while the one on the right is obtained with the Meta-Model.

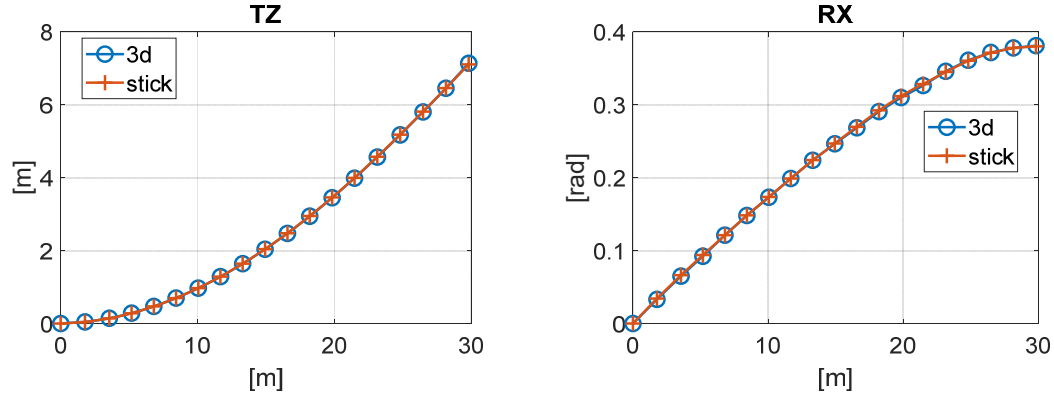


Figure 12: Displacement and rotation for force applied in Z direction, isotropic case

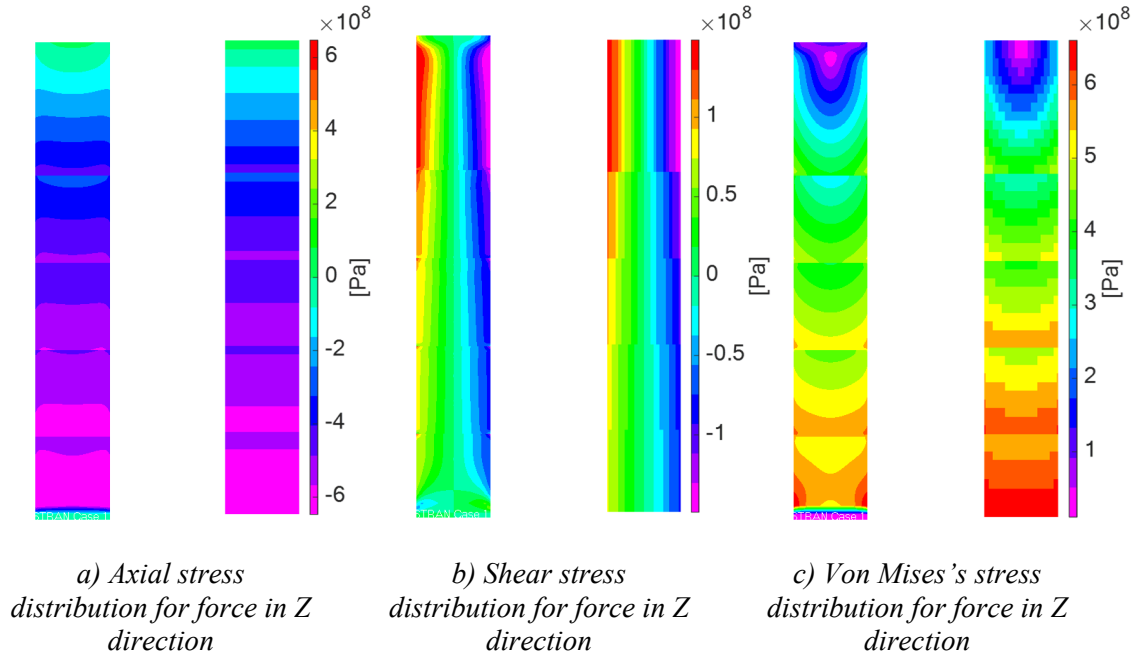


Figure 13: Stress patterns comparison for isotropic wingbox, tip load in Z direction

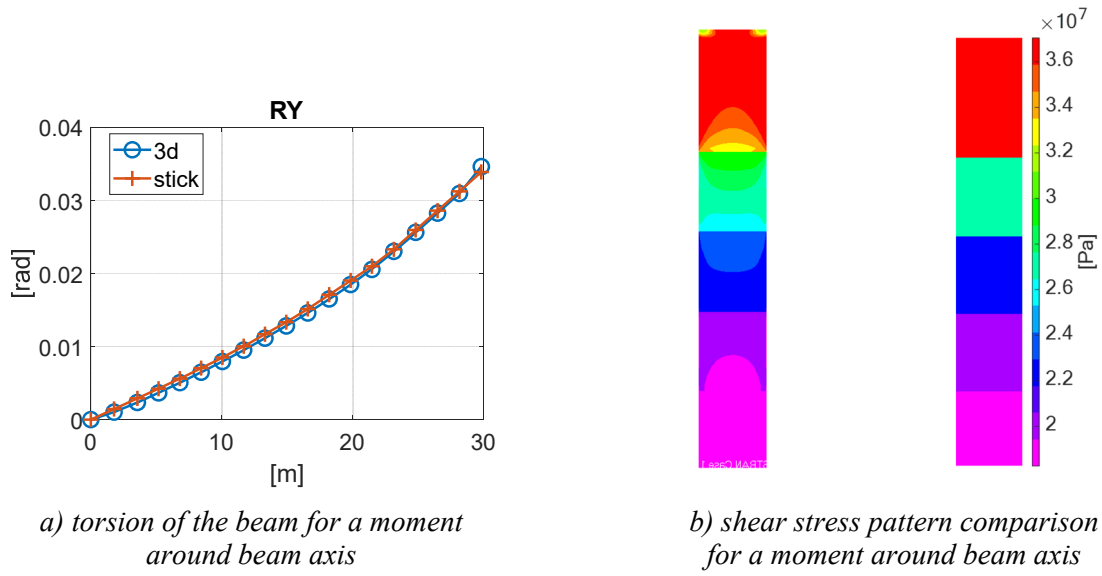


Figure 14: Comparison for a moment around beam axis

The comparisons reported in Figure 13 and Figure 14 show how the results obtained with the stick model and processed with the Meta-Model, are similar to the one obtained with the 3D FEM. The match of the deformed shapes proves that the stiffness properties are identified properly, and no information are lost passing through the cross section identification with NeoANBA. The stress distribution is recovered with a good accuracy, minor differences are present where there is a material discontinuity or a boundary condition (constraints on the root and load application on the free end). The two tests validate the Meta-Model approach when isotropic materials are adopted, but the same results could be obtained with analytical formulation. The significant advantage of NeoANBA is achieved when non-homogeneous materials are employed in the components. The example of Figure 11 is modified using unidirectional plies for the upper and lower skins, which have an orientation of 30° with respect to the beam axis. This kind of lamination for the two skins generates a bending-torsion coupling, meaning that an out of plane force generates a torsion of the beam (RY) in addition to the out of plane displacement (TZ) and rotation (RX).

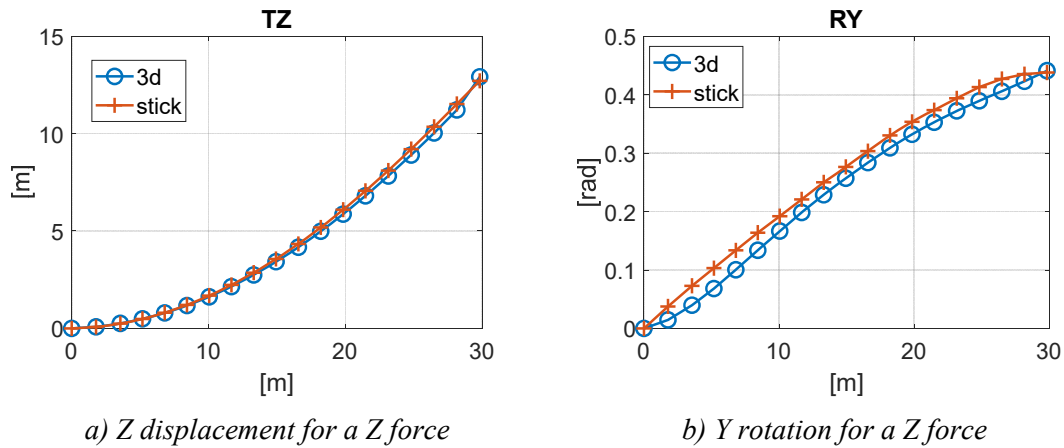


Figure 15: Displacement and rotation for force applied in Z direction, orthotropic case

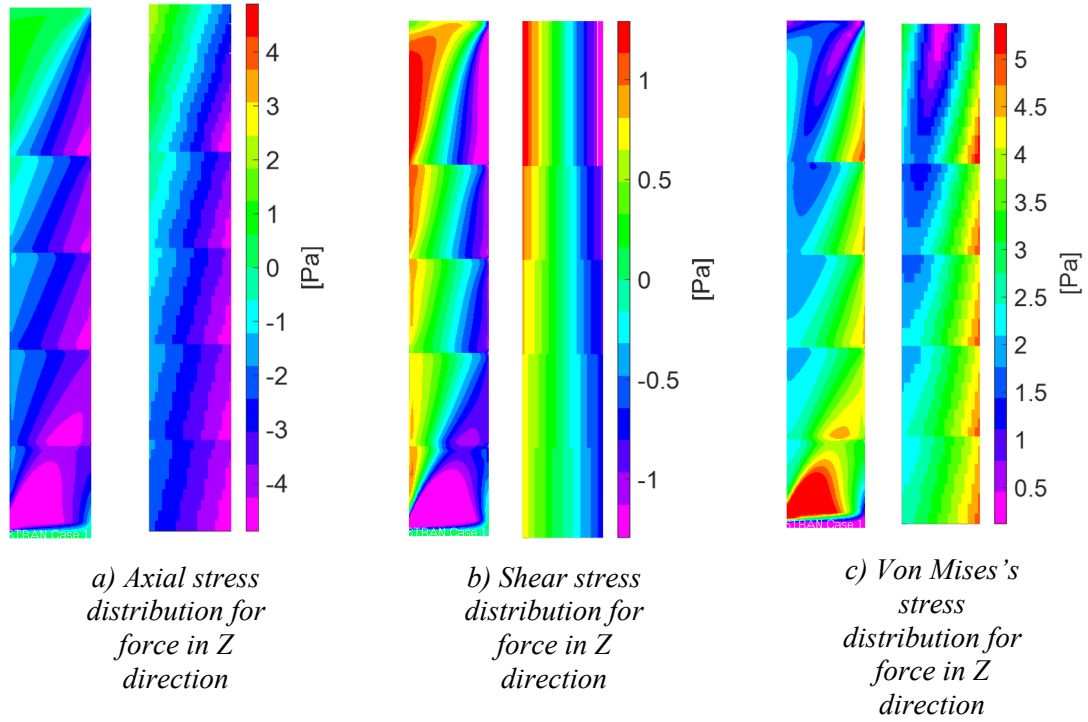


Figure 16: Stress patterns comparison for orthotropic wingbox, tip load in Z direction

The latest comparison shows that NeoANBA properly evaluates the stiffness properties of a composite thin-walled hollow section, Figure 15 shows how an out of plane force generates a torsion of the beam, the rotation has a constant offset with respect to the 3D solution, introduced in the root region by the constraint mechanism which appears to be stiffer for the 3D FEM. The offset is constant spanwise, meaning that far from the boundary condition the coupling is well matched. Figure 16 shows that the stresses are estimated in a satisfactory way as well, with small discrepancies as for the isotropic case.

It must be reminded that the stick model is suitable to perform aero-elastic analyses and it is not the most appropriate model to perform stress analyses. The Meta-Model approach improves the capability of stress evaluation of the stick-model providing a realistic stress distribution that can be used in conceptual and preliminary design phases, but it doesn't aim to substitute the 3D FEM models, which are still the reference for the detailed stress analysis. The stick model is still the reference representation of the aircraft for the load envelope computation (static trim and dynamic loads), the improvement of the wing's description provides a more realistic evaluation of the elastic behaviour and allows to fully exploit composite materials in simplified models, providing a correct evaluation of the coupling terms. This latest aspect becomes relevant when the impact of the aeroelastic tailoring (wash-in or wash-out term) [40] on the load envelopes must be evaluated.

Another relevant advantage introduced by the Meta-Model approach is the semi-analytical and multi-model representation of the component: the relationship between components and properties is fully known, hence whichever property modification is automatically mapped on all the models, which are always up to date and coherent among them and avoids condensation process. An example of the condensation process is the realization of the stick model starting from a 3D FEM model obtained after a detailed sizing, this process is automatic with the Meta-Model, but it needs a dedicated procedure when starting from a GFEM and could lead to the loss of some information during the process.

5. Application to a transport aircraft wing

In the U-HARWARD project [42], aiming at the investigation of high and ultra high aspect ratio aircraft, the Meta-Model was exploited in combination with NeoCASS to generate a family of aircraft with increasing aspect ratio, which was sized with NeOPT considering aero-elastic constraints, the results are presented in [43]. The Reference Aircraft of U-HARWARD project has selected as roughly representing the A321 aircraft and properly designed starting from the publicly available CeRas data base approximately describing the A320 aircraft. Then, this geometry was modified stretching its wing reaching a maximum Aspect Ratio of 19 as sketched in Figure 17, and each model was structurally sized and optimized to study how the fuel consumption and pollutant emissions are impacted by the increased aspect ratio. Indeed a more slender wing improves the aerodynamic performances reducing the induced drag but at the same time increases the the structural weight to withstands higher loads.

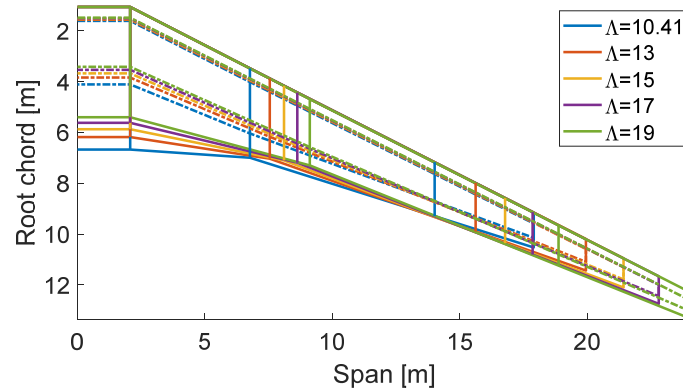


Figure 17: Wings studied in the U-HARWARD project

The optimization is performed using NeOPT [41], a newly implemented NeoCASS module able to perform a fully aeroelastic optimization problem, even in presence of active controls like load alleviation systems. The wing design variables are represented by the panel thickness and stringers area, together with possible orientation of composite elements.. A sketch of the available design variables for each wing section is represented by Figure 18 and they can be aggregated section-wise to reduce the number of design parameters. A fully symmetric wingbox can be realized imposing that upper/lower and front/aft elements have the same properties (4 design variables) or the section can be fully de-coupled having up to 10 design variables. In the example here reported the design variable used were 7 because the sizes of the spar caps were the same for the 4 elements, hence 2 thicknesses for the skins, 2 for the spars, 2 for the stringers and 1 for the spar caps. An additional level of variable linking is performed in spanwise direction where the wing is divided in patches defined by two ribs and the variables are kept equal inside the patch.

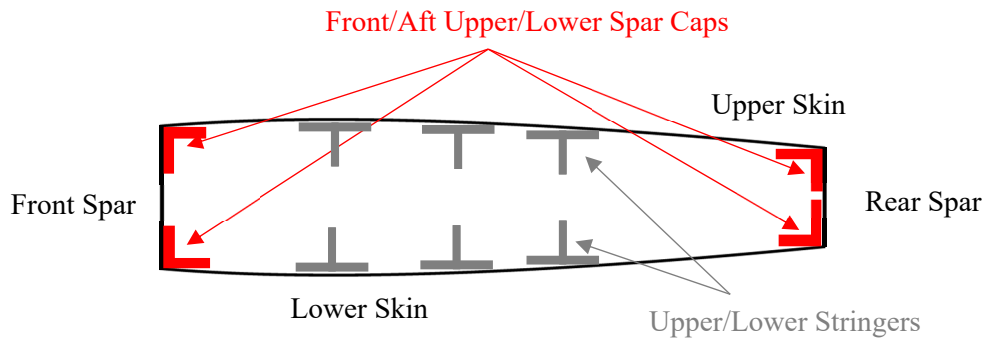


Figure 18: Cross-Section design variables

The obtained cross sections properties are translated into beam stiffness matrices through a NeoANBA cross-section model (Figure 19(d)) and updated into the aeroelastic stick model

(Figure 19(a)) that provides the aeroelastic loads to evaluate the constraints: the failure of the component is evaluated with Von Mises or Tsai-Hill criterion depending on the nature of the element, while the analytical buckling of the components is evaluated following the methods proposed in [44][45].

Through the Meta-Model it was realized the CAD model of Figure 19(b), used to create the mesh for the CFD analyses. The wingbox's detailed FEM model of Figure 19(c) will be used in the next project's phases.

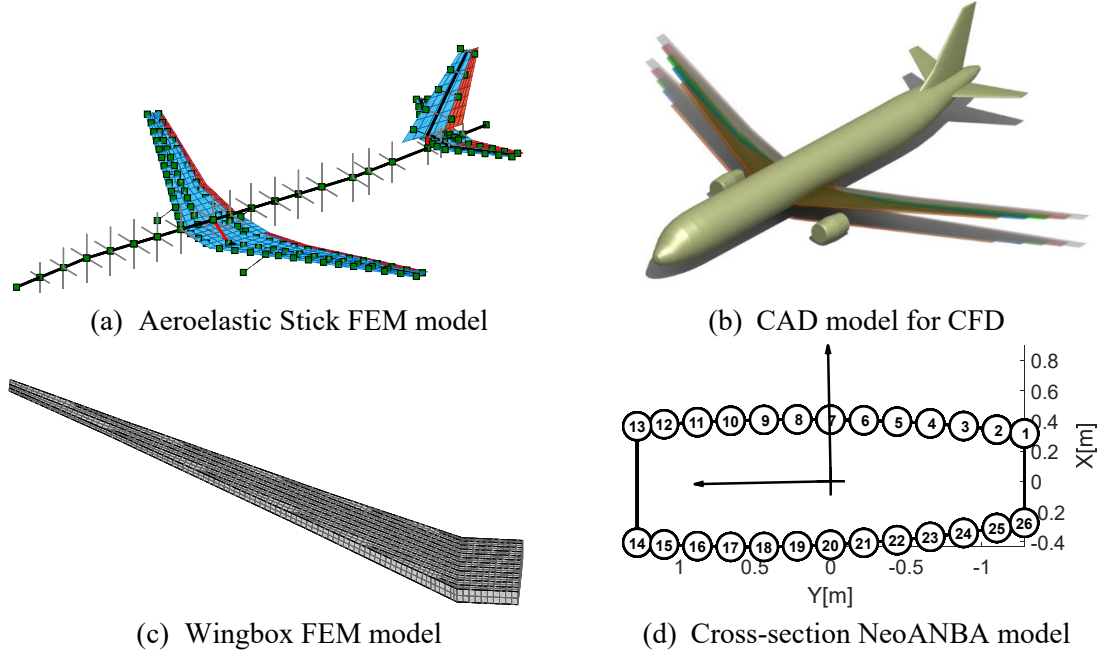


Figure 19: Model employed in the U-HARWARD project

The different disciplines involved, like structure and aerodynamics, share and interact with a common representation of the aircraft, provided by the Meta-Model. In this way, it is possible to develop different analysis models of the same discipline but with different accuracy. The aerodynamic model used for the aeroelastic computation is a DLM/VLM and it is properly coupled with the stick model by means of the radial basis functions approach, while the model used for the CFD is based on the external shape of the aircraft. Each modification, e.g. airfoil shape or twist, is automatically mapped in the two models, updating concurrently both of them. In the same way, whichever modification to the structural properties, i.e. thickness of the skin, is automatically updated in the 3D FEM model and in the stick model thanks to the re-computation of the stiffness matrix performed with NeoANBA.

The aircraft family was sized considering different trim condition (33 trim manoeuvres compliant with EASA CS25 certification rules), flutter points (3 altitudes up to 1.2Vd or 1.2Md) and 1-cos gust excitation in 2 different flight points (cruise condition at sea level and cruise altitude with 10 equally spaced gradients between 9 and 107m, both positive and negative amplitudes). The load cases are considered concurrently and the wingbox's structural mass depends on the load case selection [46].

Two different materials were considered: a classical aluminium alloy solution (AL7075-T6) and an alternative solution with a symmetric and balanced CFRP stacking sequence (Figure 20). A safety factor of 1.5 was considered on the nominal loads in the constraints computation.

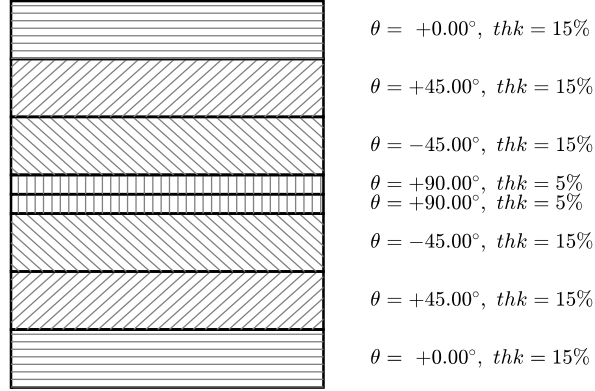


Figure 20: Symmetric and balanced stacking sequence

The result of the sizing procedure is the evolution of the wingbox structural mass with respect to the aspect ratio. Defining a prescribed amount of fuel (14037kg), a constant C_{D0} term of 0.005, an Oswald factor of $\xi = 0.9$ for the induced drag computation as $C_{di} = \frac{C_L^2}{\pi \lambda \xi}$ for the equilibrium point in the middle of the cruise $W_{CL} = 0.5(W_1 + W_2)$, it is possible to solve the Breguet's equation to obtain an indication of the range of the sized aircraft.

	AR	Half wingbox Mass [kg]	Full A/C Mass [kg]	W1 [kg]	W2 [kg]	Range [km]
AL7075-T6	10.41	2193.48	87526.05	87526.05	73489.05	3784.68
	13	2337.73	89365.53	89365.53	75328.53	4244.89
	15	2601.41	91305.23	91305.23	77268.23	4515.19
	17	2916.46	93492.07	93492.07	79455.07	4726.70
	19	3975.49	97251.43	97251.43	83214.43	4801.60
CFRP	10.41	1402.37	85943.81	85943.81	71906.81	3889.44
	13	1685.21	88060.50	88060.50	74023.50	4334.03
	15	2076.37	90255.13	90255.13	76218.13	4586.95
	17	2449.30	92557.75	92557.75	78520.75	4789.94
	19	2882.44	95065.32	95065.32	81028.32	4945.50

Table 2: Optimization results

Table 2 shows the results obtained, for both the material configurations the wingbox mass increases with the aspect ratio, but at the same time the range with a fixed amount of fuel increases as well, meaning that it is needed less fuel for a given route. The increased structural weight worsens the structural efficiency, but the aerodynamic performance increase compensates this effect, improving the overall performance of the aircraft with an increased wingspan.

This flexible and automated procedure helps the designers to understand how the modification of each parameter impacts on the performances, automatically updating all the models involved in the design cycle at conceptual level. The data-management reduces the design time, providing a fully automated procedure where the user does not have neither to re-create nor update a FEM model when a modification is applied.

6. The meta-model as a Digital Twin

The most recent definition of the DT is provided by AIAA in [47]: “A set of virtual information constructs that mimics the structure, context and behaviour of an individual / unique physical

asset, or a group of physical assets, is dynamically updated with data from its physical twin throughout its life cycle and informs decisions that realize value.”

From an historical perspective, the first DT was realized by NASA during the Apollo program, even if it wasn't called with this name. It consisted in a digital simulator ground based in Huston which would mimic the mission, feeding the real time data into the simulator. This was crucial to rescue the Apollo 13 crew, driving the NASA's decision-making process with physically based simulation based on telemetry data. It was possible to evaluate different manoeuvres and scenarios for the re-entry orbit and to simulate different solutions to control the CO₂ concentration in the spacecraft after the accident.

The authors' view of the Digital Twin is a modular approach where each component, starting from the whole aircraft, is associated with a set of Computer Aided Engineering Models (CAEMs). The CAEMs are models that describe single/multi physics problems related to a single/multiple components, they receive inputs and provide outputs from/to CAEMs of other discipline or components. This last aspect is represented by the double-ended arrows in the block diagram of Figure 21, meaning that the results obtained with a model are processed and fed to other models to obtain other results in other disciplines.

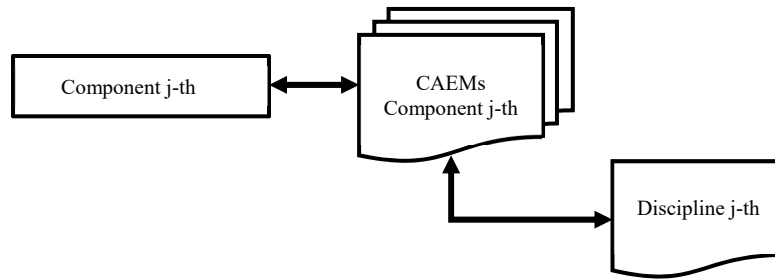


Figure 21: Basic Digital Twin block

The Digital Twin is an entity which dimensions and complexity depends by the integration level achieved in the model management system. Narrowing its application to the models available with the Meta-Model approach, it is possible to build a DT oriented on the aero-servo-elastic disciplines for the whole aircraft, with an increased detail and complexity for the wingbox. With the Meta-Model there are available many models:

The Aero-Elastic Stick Model (AESM) of the complete aircraft, which is used in its Finite Element (FE) or State-Space (SS) form by NeoCASS to perform aero-servo-elastic analyses. In the AESM(SS) it is possible to embed the Dynamic Models (DMs) of the actuation systems.

For the wingbox subcomponent there are available a Stress Analysis Model (SAM) that is the 3D FEM model, the cross-sectional model of NeoANBA and the CAD model.

The block diagram of the Digital Twin generated with the approach proposed is illustrated in Figure 22, where all the elements are presented. The input/output relationship are established by the user depending on which results are required. An example is the recovery of the stress experienced by the wing during a mission: the set of manoeuvres and dynamic load conditions are reproduced with the AESM, the results in term of internal forces are transformed into a set of static loads and applied to the wingbox's SAM. The results in term of stresses are used to evaluate the impact of the mission on the fatigue life, adapting the maintenance interval of the components in real time and for each aircraft.

The effect of the fatigue on the materials can be a modification of their properties, the Digital Twin allows to modify almost in real time these variations and evaluate how the aeroelastic response is affected. Moreover, in a rolling-wave approach, the updated materials provide a new estimation of the useful life of the aircraft components which is translated into a re-scheduling of the maintenance operations.

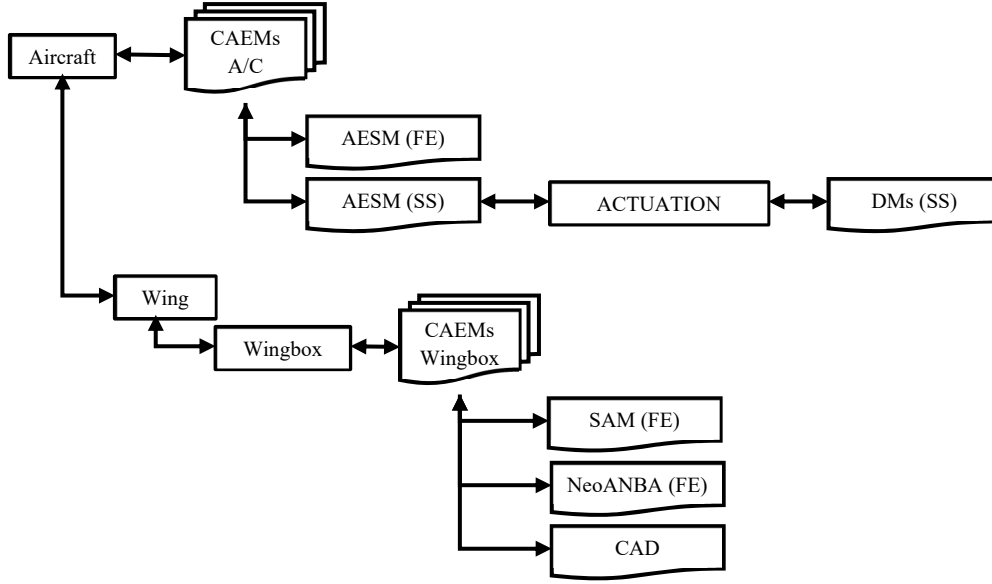


Figure 22: Digital Twin representation of the meta-model

7. Conclusions

This work presented a highly accurate approach to the wingbox description to be used in aircraft conceptual and preliminary design phases. Indeed, the Meta-Model provides an accurate geometrical representation of the wingbox, which is automatically translated into different analysis models, like the stick-model for aero-servo-elastic analyses, the cross-section FE model for stiffness and mass matrices evaluation and the 3D GFEM of the wingbox. The semi-analytical formulation of the Meta-Model does not lose the coherence among the models, which is a key factor to automatically update all the models with a single operation. This latest feature assumes a relevant advantage avoiding condensation or model reduction procedure because the Meta-Model automatically maps the properties among the different models.

When compared with the results obtained with a detailed model, the ones obtained with the stick model based on structural properties derived from the sectional solver, are well correlated, even if some difference in the stress pattern are present indeed. It must be pointed out that the Meta-Model (10 to 30 nodes typically for a half wing) does not aim to substitute the detailed GFEM (>10000 nodes) for the stress analyses, but its role is to improve the stress recovery obtained from aero-servo-elastic analysis and optimization loop performed with a stick model, together with the fully capturing of structural couplings typical of advanced composites.

The structural Meta-Model proposed here not only far surpasses what is available in normal conceptual design tools, but also allows global tradeoff analyses capable of evaluating the impact of an advanced use of composites from the earliest stages of the design. Design philosophies such as the aeroelastic tailoring, especially if based on fiber placement methodologies, can in fact be fully implemented and assessed in terms of impact on the high-level aircraft performances, such as fuel burn and emissions.

With a wider view, the Meta-Model here presented and especially built for the conceptual and preliminary design phases can be seen as the first brick of a possible Digital Twin (DT) of the aircraft. In fact, it allows to generate different purpose and multi-physics coherent models (CAEMs) of the whole aircraft and its sub-components, opening the possibilities of developing a DT associated to each tail number to perform a real time monitoring of the health status of an aircraft during its lifecycle.

Acknowledgements

The U-HARWARD Project has received funding from the Clean Sky 2 Joint Undertaking, under the European's Union Horizon 2020 research and innovation Program

under Grant Agreement number: 886552 - H2020 -CS2-CFP10-2019-01. The continued support of Gian Luca Ghiringhelli is highly appreciated.

Data availability

Data are available on request, please contact francesco.toffol@polimi.it

References

- [1] A. Kharina and D. Rutherford, "Fuel efficiency trends for new commercial jet aircraft: 1960 to 2014," 2015
- [2] A. Jameson, "Re-engineering the design process through computation," *Journal of Aircraft*, vol. 36, no. 1, pp. 36–50, 1999.
- [3] W. G. Roeseler, B. Sarh, M. U. Kismarton, J. Quinlivan, J. Sutter, and D. Roberts, "Composite structures: the first 100 years," in *16th International Conference on Composite Materials*, pp. 1–41, Japan Society for Composite Materials Kyoto, Japan, 2007.
- [4] E. Commision, "Flightpath 2050 Europe's vision for aviation." <https://ec.europa.eu/transport/sites/transport/files/modes/air/doc/flightpath2050.pdf>, 2011.
- [5] R. Jansen, C. Bowman, A. Jankovsky, R. Dyson, and J. Felder, "Overview of nasa electrified aircraft propulsion (eap) research for large subsonic transports," in *53rd AIAA/SAE/ASEE Joint Propulsion Conference*, p. 4701, 2017.
- [6] Sohst, Martin, et al. "Optimization and comparison of strut-braced and high aspect ratio wing aircraft configurations including flutter analysis with geometric non-linearities." *Aerospace Science and Technology* (2022): 107531.
- [7] A. Frediani, V. Cipolla, and E. Rizzo, "The prandtlplane configuration: overview on possible applications to civil aviation," *Variational Analysis and Aerospace Engineering: Mathematical Challenges for Aerospace Design*, pp. 179–210, 2012.
- [8] R. Cavallaro, R. Bombardieri, L. Demasi, and A. Iannelli, "Prandtlplane joined wing: Body freedom flutter, limit cycle oscillation and freeplay studies," *Journal of Fluids and Structures*, vol. 59, pp. 57–84, 2015.
- [9] R. H. Liebeck, "Design of the blended wing body subsonic transport," *Journal of aircraft*, vol. 41, no. 1, pp. 10–25, 2004.
- [10] Z. Lyu and J. R. Martins, "Aerodynamic design optimization studies of a blended-wing-body aircraft," *Journal of Aircraft*, vol. 51, no. 5, pp. 1604–1617, 2014.
- [11] W. Su and C. E. Cesnik, "Nonlinear aeroelasticity of a very flexible blended-wing-body aircraft," *Journal of Aircraft*, vol. 47, no. 5, pp. 1539–1553, 2010.
- [12] T. Delft, "Flying v." <https://www.tudelft.nl/en/ae/flying-v/>.
- [13] D. Raymer, *Aircraft design: a conceptual approach*. American Institute of Aeronautics and Astronautics, Inc., 2012.
- [14] E. Torenbeek, *Synthesis of subsonic airplane design: an introduction to the preliminary design of subsonic general aviation and transport aircraft, with emphasis on layout, aerodynamic design, propulsion and performance*. Springer Science & Business Media, 2013.
- [15] L. Cavagna, S. Ricci, and L. Travaglini, "Neocass: an integrated tool for structural sizing, aeroelastic analysis and mdo at conceptual design level," *Progress in Aerospace Sciences*, vol. 47, no. 8, pp. 621–635, 2011.
- [16] L. Cavagna, S. Ricci, and L. Travaglini, "Structural sizing and aeroelastic optimization in aircraft conceptual design using neocass suite," in *13th AIAA/ISSMO Multidisciplinary Analysis Optimization Conference*, p. 9076, 2010.
- [17] L. Cavagna, S. Ricci, and L. Riccobene, "A fast tool for structural sizing, aeroelastic analysis and optimization in aircraft conceptual design," in *50th AIAA/ASME/ASCE/AHS/ASC Structures, Structural Dynamics, and Materials Conference 17th AIAA/ASME/AHS Adaptive Structures Conference 11th AIAA No*, p. 2571, 2009.

- [18] L. Cavagna, S. Ricci, and L. Riccobene, "Structural sizing, aeroelastic analysis, and optimization in aircraft conceptual design," *Journal of Aircraft*, vol. 48, no. 6, pp. 1840–1855, 2011.
- [19] N. Werter and R. De Breuker, "A novel dynamic aeroelastic framework for aeroelastic tailoring and structural optimisation," *Composite Structures*, vol. 158, pp. 369–386, 2016.
- [20] You, Chao, et al. "Identification of the key design inputs for the FEM-based preliminary sizing and mass estimation of a civil aircraft wing box structure." *Aerospace Science and Technology* 121 (2022): 107284.
- [21] Hürlimann, Florian, et al. "Mass estimation of transport aircraft wingbox structures with a CAD/CAE-based multidisciplinary process." *Aerospace Science and Technology* 15.4 (2011): 323-333.
- [22] B. A. Autry and D. Victorazzo, "Automated top level aircraft structural sizing tool (atlass): A framework for preliminary aircraft design and optimization," in *AIAA Scitech 2019 Forum*, p. 0550, 2019.
- [23] P. Piperni, A. DeBlois, and R. Henderson, "Development of a multilevel multidisciplinary optimization capability for an industrial environment," *AIAA journal*, vol. 51, no. 10, pp. 2335–2352, 2013.
- [24] van Dooren, K. S., Tijs, B. H. A. H., Waleson, J. E. A., & Bisagni, C. (2023). Skin-stringer separation in post-buckling of butt-joint stiffened thermoplastic composite panels. *Composite Structures*, 304, 116294.
- [25] Oliveri, V., Zucco, G., Peeters, D., Clancy, G., Telford, R., Rouhi, M., ... & Weaver, P. M. (2019). Design, manufacture and test of an in-situ consolidated thermoplastic variable-stiffness wingbox. *AIAA Journal*, 57(4), 1671-1683.
- [26] Liguori, F. S., Zucco, G., Madeo, A., Magisano, D., Leonetti, L., Garcea, G., & Weaver, P. M. (2019). Postbuckling optimisation of a variable angle tow composite wingbox using a multi-modal Koiter approach. *Thin-Walled Structures*, 138, 183-198.
- [27] Zucco, G., Oliveri, V., Rouhi, M., Telford, R., Clancy, G., McHale, C., ... & Peeters, D. (2020). Static test of a variable stiffness thermoplastic composite wingbox under shear, bending and torsion. *The Aeronautical Journal*, 124(1275), 635-666.
- [28] Tuegel, E. (2012, April). The airframe digital twin: some challenges to realization. In *53rd AIAA/ASME/ASCE/AHS/ASC structures, structural dynamics and materials conference 20th AIAA/ASME/AHS adaptive structures conference 14th AIAA* (p. 1812).
- [29] Glaessgen, E., & Stargel, D. (2012, April). The digital twin paradigm for future NASA and US Air Force vehicles. In *53rd AIAA/ASME/ASCE/AHS/ASC structures, structural dynamics and materials conference 20th AIAA/ASME/AHS adaptive structures conference 14th AIAA* (p. 1818).
- [30] Tuegel, E. J., Ingrassia, A. R., Eason, T. G., & Spottswood, S. M. (2011). Reengineering aircraft structural life prediction using a digital twin. *International Journal of Aerospace Engineering*, 2011.
- [31] G. Bindolino, G. Ghiringhelli, S. Ricci, and M. Terraneo, "Multilevel structural optimization for preliminary wing-box weight estimation," *Journal of Aircraft*, vol. 47, no. 2, pp. 475–489, 2010.
- [32] T. Möller, "A fast triangle-triangle intersection test," *Journal of graphics tools*, vol. 2, no. 2, pp. 25–30, 1997.
- [33] J. Tuszynski, "Surface intersection." <https://www.mathworks.com/matlabcentral/fileexchange/48613-surface-intersection>, 2020.
- [34] Piegl, L., & Tiller, W. (1996). *The NURBS book*. Springer Science & Business Media.
- [35] Toffol, F., and S. Ricci. "Wingbox Meta-Model and Aero-Servo-Elastic Optimization With NEOPT." *International Conference on Multidisciplinary Design Optimization of Aerospace Systems (AeroBest 2021)*. IDMEC, 2021.
- [36] V. Giavotto, M. Borri, P. Mantegazza, G. Ghiringhelli, V. Carmaschi, G. Maffioli, and F. Mussi, "Anisotropic beam theory and applications," *Computers & Structures*, vol. 16, no. 1-4, pp. 403–413, 1983.
- [37] Giavotto, V. (1977) *Strutture aeronautiche*. Clup.
- [38] Mantegazza, P. (1977) *Analysis of semimonocoque beam sections by the displacement method*, *L'Aerotecnica Missili e Spazio*, pp. 179–182
- [39] Cesnik, C. E., & Hodges, D. H. (1997). VABS: a new concept for composite rotor blade cross-sectional modelling. *Journal of the American helicopter society*, 42(1), 27-38.
- [40] C. V. Jutte and B. K. Stanford, *Aeroelastic tailoring of transport aircraft wings: state-of-the-art and*

potential enabling technologies. National Aeronautics and Space Administration, Langley Research Center, 2014.

- [41] Toffol, F. (2021). *Aero-servo-elastic optimization in conceptual and preliminary design*, PhD Thesis, Politecnico di Milano, 2021
- [42] Ricci, Sergio, et al. "U-HARWARD: a CS2 EU funded project aiming at the Design of Ultra High Aspect Ratio Wings Aircraft." *AIAA Scitech 2022 Forum*. 2022.
- [43] Ricci, S., Marchetti, L., Toffol, F., Beretta, J., & Paletta, N. (2022). *Aeroelastic Optimization of High Aspect Ratio Wings for Environmentally Friendly Aircraft*. In *AIAA SCITECH 2022 Forum* (p. 0166).
- [44] P. M. Weaver and M. P. Nemeth, "Bounds on flexural properties and buckling response for symmetrically laminated composite plates," *Journal of engineering mechanics*, vol. 133, no. 11, pp. 1178–1191, 2007.
- [45] J. E. Herencia, P. M. Weaver, and M. I. Friswell, "Optimization of long anisotropic laminated fiber composite panels with t-shaped stiffeners," *AIAA journal*, vol. 45, no. 10, pp. 2497–2509, 2007.
- [46] Binder, Simon, Andreas Wildschek, and Roeland De Breuker. "The interaction between active aeroelastic control and structural tailoring in aeroservoelastic wing design." *Aerospace Science and Technology* 110 (2021): 106516.
- [47] *ALAA Digital Engineering Integration Committee*. (2020). *Digital Twin: Definition & Value—An ALAA and AIA Position Paper*. ALAA: Reston, VA, USA.